Birthdays of retinal amacrine cell subtypes are systematically related to their molecular identity and soma position

Paula E. Voinescu, **Jeremy N. Kay**, and **Joshua R. Sanes**
Department of Molecular and Cellular Biology and Center for Brain Science, Harvard University, Cambridge MA, 02138 USA

Abstract

The mammalian retina contains six major cell types, several of which are divided into multiple molecularly and morphologically distinct subtypes. To understand how subtype diversity arises during development, we focused on amacrine interneurons in the mouse retina; ~30 amacrine subtypes have been identified in mammals. We used antibody markers to identify the two main amacrine subsets – GABAergic and glycinergic – and further subdivided these groups into smaller subsets based on expression of neurotransmitter and transcription factor markers. We then used bromodeoxyuridine (BrdU) labeling to ask whether amacrine subsets are born (become postmitotic) at different times, as is the case for lamina-specified subsets of cortical projection neurons. We found that GABAergic amacrines are generated on average 2–3 days before glycinergic amacrines. Moreover, subsets of GABAergic amacrines are born at distinct times. We also found a strong correlation between amacrine cell birthday and soma position in the mature retina, another point of similarity with cortical projection neurons. This relationship raised the possibility that amacrine subtype identity is determined by signals that uncommitted cells receive after they migrate to their destinations. However, cells labeled with BrdU *in vivo*, then dissociated and allowed to develop *in vitro*, acquired the amacrine subtype-specific markers appropriate for their birthdays, supporting the idea that they become specified near the time and place of their birth. Together, our results suggest that the birthdays of amacrine cells independently specify their destinations and subtype identities.

Keywords

INTRODUCTION

The remarkable capabilities of the nervous system result from precise interactions among diverse neuronal cell types. The vertebrate retina is a good example of such variety: although it contains only six main neuronal types, these can be divided into over 60 separate morphologically distinct subtypes (Masland, 2001). Yet, all these cells arise from a relatively small pool of multipotent progenitors. How can these progenitors generate such a variety of cell types?

There are several mechanisms for diversification of progenitor cells and their progeny that are conserved through evolution, at least in broad outlines, and each has been implicated in neural cell fate specification. In the vertebrate spinal cord, for example, gradients of soluble morphogens pattern expression of transcription factors that in turn determine cell fate (Dalla

Correspondence to: Joshua R. Sanes Department of Molecular and Cellular Biology Center for Brain Science Harvard University 52 Oxford Street Cambridge MA 02138 Phone: 617-496-8683 FAX: 617-495-0524 sanesj@mcb.harvard.edu.

Torre di Sanguinetto et al., 2008; Gurdon and Bourillot, 2001; Jessell, 2000). In *Drosophila* retina, local interactions among initially equivalent cells lead to diversification of photoreceptors (Voas and Rebay, 2004), while within *Drosophila* neuroblast pool, lineage dictate cell fate (Brody and Odenwald, 2002). And in mammalian cerebral cortex, the timing of cell cycle exit – neuronal birthdate – plays a major role in subtype identity; extrinsic determinative factors and the ability of progenitors to respond to these factors both change as a function of time, leading to a dependence of laminar cell type identity on birth order (Molyneaux et al., 2007).

The mode of cell type diversification in the retina is currently thought to be most similar to that in cortex. Indeed, the six main retinal cell types have distinctive, although overlapping, birthdates (Harman and Beazley, 1989; Holt et al., 1988; Hu and Easter, 1999; Kahn, 1974; La Vail et al., 1991; Rapaport et al., 2004; Sidman, 1961; Young, 1985a; Zimmerman et al., 1988). Although cell lineage may play some role in specification of these cells (Cayouette et al., 2003; Cayouette et al., 2006), analysis of temporally varying intrinsic and extrinsic determinants of retinal cell fate led Cepko to propose that progenitors pass through different competence states over the course of development. In each state, multipotent cells can only give rise to a limited set of progeny, leading to production of distinct cell types in order (Cayouette et al., 2006; Cepko et al., 1996; Livesey and Cepko, 2001).

Almost completely unexplored is the issue of how the main retinal cell types diversify to acquire distinct subtype identities. Here, we address this question with respect to amacrine cells, interneurons that modulate the information transmitted from bipolar to ganglion cells. Amacrine cells are the most diverse neuronal class of the retina, with 30 or more distinguishable morphological subtypes (MacNeil et al., 1999; MacNeil and Masland, 1998). Despite their morphological diversity, the vast majority of amacrine cells are inhibitory interneurons (Masland, 2001; Schubert et al., 2008; Wassle et al., 1998), and they are often divided into two groups based on whether they use GABA or glycine as their inhibitory neurotransmitter. Using the BrdU method (Packard et al., 1973), we show that GABAergic and glycinergic amacrines in mouse retina become postmitotic at overlapping, but distinct times. We then use additional markers to show that at least the GABAergic population comprises discrete subpopulations with distinct birthdays. Thus, the relationship of birthdate to cell fate, long known for the main retinal cell types, extends to at least some subtypes.

In analyzing these data, we noted that the time at which amacrines are born in the neuroblast layer is correlated with the position to which its soma migrates, a relationship reminiscent of that in cortex (Leone et al., 2008; McConnell, 1985; Metin et al., 2006; Molyneaux et al., 2007; Shen et al., 2006). Consideration of this relationship led us to wonder whether amacrine cells acquire their subtype-specific identity around the time they are generated, as occurs in cortex and for the broad retinal neuron classes, or as a consequence of signals received at their destination, as may occur in the peripheral sensory and autonomic nervous system (Edlund and Jessell, 1999). We designed experiments to distinguish these alternatives, results of which show that at least some amacrine subtypes are specified near the time of their birth.

MATERIALS AND METHODS

Animals

Timed pregnant mice (CD1 and C57/B6) were purchased from Charles River, Wilmington, MA, or bred in our colony. The presence of a vaginal plug marked embryonic day 0 (E0) and the accuracy of the timing was verified by noting the day of birth, which was presumed to be 18.5 days from conception.

Bromodeoxyuridine (BrdU), (Sigma, St. Louis, MO) was prepared in 10mM Tris buffer, pH 7.4. Timed pregnant female or mouse pups were injected subcutaneously in the neck with a single dose of BrdU (50 μg per gram of body weight). Mice were euthanized at postnatal day (P) 14 or 15 by an overdose of Nembutal (pentobarbital) injected intraperitoneally. We analyzed retinas from three to nine animals for each injected embryonic age (E8, E10, E12, E14, E17) and from two to four animals for each injected postnatal age (P0, P1, P3, P5, P6). For studies in vitro, pregnant females were injected with BrdU at E12 or E17, then pups were sacrificed at P0.

Histology

Eyes were collected and fixed for 15–20 min in 4% paraformaldehyde (PFA), then the cornea was cut along the ora serrata and the anterior part of the eye was removed. The retina, preserved in the optic cup, was fixed for 30–45 additional minutes in 4% PFA, incubated for 2h in 30% sucrose/PBS, frozen in Tissue Freezing Medium (Triangle Biomedical Sciences), and sectioned at 20μm in a cryostat.

Sections were incubated in PBS for 10min at room temperature, and 2N HCl for 30min at 37 °C, for antigen retrieval. Following two 5 min washes in 0.1M sodium borate, pH 8.5, and a rinse in PBS, sections were incubated successively in blocking solution (3% donkey serum/ 0.3% Triton X-100/PBS) for 30 min at room temperature, primary antibodies overnight at 4 °C, and Alexa-conjugated secondary antibodies (Molecular Probes) for 1–2 h at room temperature. Sections were then washed thoroughly with PBS, coverslipped with Biomeda mounting media, and imaged on an Olympus FV1000 scanning confocal microscope or a Zeiss LSM 5 Pascal confocal microscope. Primary antibodies are listed in Table 1.

Antibody characterization

Primary antibodies used in this study are listed in Table 1.

The antibody to Brn-3a (Chemicon) labels only RGCs in retinas of several vertebrate species including mouse (Gerrero et al., 1993; Xiang et al., 1995). According to the manufacturer, it does not recognize Brn-3b or Brn-3c and does not stain tissue from Brn-3a knock-out mice.

The antibody to Chx10 (Exalpha) stains retina in a pattern consistent with that reported previously (Elshatory et al., 2007); (Liu et al., 1994). According to the manufacturer, it recognizes only the expected 46-kDa band in a retinal lysate from adult mouse tissue.

The antibody to syntaxin-1 (HPC-1; Sigma) was produced against the crude membrane fraction of the rat hippocampus and identified as a specific marker of retinal amacrine cells (Barnstable et al., 1985). It was shown to recognize syntaxin-1 protein by Inoue et al. (1992). The staining pattern we observed was indistinguishable from that reported is previous studies (Li et al., 2004).

The antibody to choline acetyl transferase (ChAT; Chemicon) detects a single 68–72-kDa band on immunoblots (Brunelli et al., 2005). It labels only cholinergic neurons in the striatum as shown by abrogation of staining following immunodepletion of cholinergic neurons (Kitabatake et al., 2003). The staining pattern we observed was indistinguishable from that reported is previous studies (Elshatory et al., 2007).

The antibody to neuropeptide Y (NPY; Bachem) has been used in studies of NPY knockout mice. It stains specific subsets of neurons in wild-type mice but not in NPY mutants (Ste Marie et al., 2005).

The antibody to tyrosine hydroxylase (TH; Chemicon) stains retina in a pattern identical to that reported previously (Haverkamp and Wassle, 2000). According to the manufacturer, it recognizes a single band at approximately 62kDa on immunoblots.

The antibody to glutamate decarboxylase (GAD65/67; Chemicon) recognizes products of both the GAD65 and the GAD67 genes. It stains retina in a pattern similar to that reported for other antibodies to the same antigen. According to the manufacturer, it recognizes only the expected doublet at 65–68 kDa on Western blots of adult brain lysates, and immunohistochemical is abolished by preincubation with corresponding immunogen peptide (Chemicon AG252).

The antibody to the Glycine Transporter 1 (GlyT1; Chemicon) stained retinas in patterns indistinguishable from those reported in previous studies (Rice and Curran, 2000). In brain, it stains in patterns corresponding to those described using in situ hybridization with probes to GlyT1 mRNA. According to the manufacturer, preabsorption of the antibody with the immunogen peptide completely abolishes the immunostaining.

The antibody to VGlut3 (Chemicon) stains brain in patterns corresponding to those described using in situ hybridization with probes to VGlut3 mRNA. This staining pattern also coincides with the described distribution of immunoreactivity obtained with other VGlut3 antisera (Fremeau et al., 2002; Gras et al., 2002; Haverkamp and Wassle, 2004; Johnson et al., 2004; Schafer et al., 2002). According to the manufacturer, preabsorption of the antiserum with the immunogen peptide (Chemicon AG320) eliminates all immunostaining.

An antibody to the Ebf transcription factors was generously provided by R. Reed (Johns Hopkins University; (Davis and Reed, 1996). The authors showed that the antibody stains in patterns corresponding to those obtained by in situ hybridization. The antibody cross-reacts with Ebf-3 and may cross-react with Ebf-2, which had not been identified at the time the antibody was generated (R. Reed, personal communication). We therefore refer to this antibody as "anti-Ebf."

For all primary antibodies, features pointed out as positive staining were not seen in the absence of the primary antibody.

Secondary antibodies were obtained from Jackson ImmunoResearch Lab, West Grove, PA, or Molecular Probes.

Cell culture

Retinal cells were cultured using the protocol described by Lefebvre et al. (2008). Briefly, P0 retinas were dissociated with papain and plated onto poly-D-lysine coated 8-well Permanox chamber slides (Nunc) in Neurobasal supplemented with BDNF and B27. Cells were cultured for 9 days, with a change of medium 5, then fixed with 4% paraformaldehyde/4% sucrose for 15 minutes, and immunostained.

Cell counting and statistical analysis

Sections through and near the optic nerve head were used for analysis. Images were taken in central retina, approximately 500μm from the optic nerve head, and in the periphery, approximately 500μm from ora serrata. To estimate population sizes for each amacrine subset we counted only the amacrines in central sections. This may explain why some data in Table 2 differ from those in (Jeon et al., 1998). Abercrombie's correction factor was applied for each count, taking into account the mean nuclear diameter for each subtype of amacrine cells (Guillery, 2002).

Retinal sections were double or triple immunostained with antibodies against BrdU and markers of interest, and the percentage of marker-positive cells also positive for BrdU was determined for each time point. BrdU-positive nuclei were followed and counted in each optical section of the confocal images to identify cells undergoing their last S-phase during the time that BrdU was available. Based on published work, we estimate that BrdU is available for approximately 2–3 hours following injection (Packard et al., 1973). The statistical significance of differences among subtypes at each time point were determined by Students t-test for means, performed on the raw data, as well as on the normalized and cumulative values. Cumulative curves were further analyzed by calculating a 90% confidence interval for each time point.

Several limitations to the birthdating data need to be acknowledged. First, because we analyzed retinas at P14, following the period of naturally occurring amacrine cell death (Pequignot et al., 2003; Young, 1984), our results refer only to cells that survived this period. Second, although we counted only intensely labeled BrdU-positive cells, we may have included some cells that divided twice following BrdU injection. These uncertainties may influence the absolute values reported, but they are unlikely to affect the significance of differences among populations, because errors would equally affect all cell types. Third, because the length of the S-phase increases progressively throughout retinogenesis (Alexiades and Cepko, 1996; Young, 1985b), the tails of the birthdating curves may be shorter than our estimates here, so separation among later born subsets may be greater than shown.

To estimate soma position, we divided the inner half of the inner nuclear layer (INL), where amacrines reside, in thirds; we then counted the number of nuclei for each subset in each region. This division was based on the approximate thickness of the inner nuclear layer, which in central retina consists of about six rows of cell nuclei, the innermost three containing mostly amacrine cells, and the outermost containing mostly bipolar and horizontal cells. The advantage of this method, as opposed to directly counting the row of nuclei, is that it does not require that sections be perfectly perpendicular to the inner nuclear layer. Counts were done on sections labeled with the subset marker and a nuclear marker, TO-PRO3 (633 nm excitation, Molecular Probes). We calculated a weighted average of these positions to find the mean row for the soma position of each subset.

RESULTS

Amacrine cells are born over a protracted period

Previous studies have documented birthdays of the main retinal cell types in several species (see Introduction), but few data are available on mice (Sidman, 1961; Young, 1985a). Moreover, cells have generally been identified based on their nuclear position and morphology, which is prone to error. We therefore began this study by using well-established molecular markers to birthdate the three cell types with the largest number of subtypes in mouse retina – amacrine cells, bipolar cells, and retinal ganglion cells (RGCs). Syntaxin-1 is a pan-amacrine cell marker (Inoue and Akagawa, 1993; Inoue et al., 1992), Chx10 labels bipolar cells (Burmeister et al., 1996), and Brn3a tags the majority of RGCs in postnatal retina (Xiang et al., 1995). Syntaxin-1 also labels horizontal cells, but they can be easily distinguished from amacrine cells based on their position in the retina.

Pregnant females or pups were injected with BrdU at one of ten time points between embryonic day (E) 8 and postnatal day (P) 6, and were allowed a long survival time to dilute the BrdU label from continuously dividing cells. This method preferentially labels cells that undergo their final S-phase at the time of injection (see Methods). Animals were sacrificed at P14–15, a time when nearly all cells have differentiated and the markers we used are expressed at adult levels. We double-stained retinal sections with antibodies against BrdU and the marker of

interest and determined the percentage of marker-positive cells in central retina that was also BrdU-positive (Figure 1A–C).

As shown in Figure 1D, RGCs were born between E8 and E17, with a peak around E11; amacrines were born between E8 and P5, with a peak around E 16, and bipolars were generated between E17 and P6, with a peak around P2. These results are consistent with previous work on mouse retina (Sidman, 1961; Young, 1985a) and with the relative birth order (RGCs then amacrines then bipolars) documented in other species (Harman and Beazley, 1989; Kahn, 1974; La Vail et al., 1991; Rapaport et al., 2004; Zimmerman et al., 1988). Because amacrines are born over a more protracted period than either of the two others, we focused on them to test the idea that the broad distribution of birthdates of a cell type reflects the combined narrower distributions of several subtypes.

Distinct birthdates of GABAergic and glycinergic amacrine cells

Most amacrine cells form inhibitory synapses on RGCs and bipolar cells (Masland, 2001; Schubert et al., 2008; Wassle et al., 1998). The ~30 amacrine subtypes are often divided on the basis of whether they use glycine or GABA as their inhibitory neurotransmitter (Haverkamp and Wassle, 2000; Masland, 2001), although some amacrines may be neither glycinergic nor GABAergic (Strettoi and Masland, 1996). To identify these amacrine populations, we used antibodies to the glycine transporter, GlyT1, and to the GABA synthetic enzymes, GAD65 and GAD67, in parallel with syntaxin-1, the pan amacrine marker (Figure 2A–B). We found that anti-GAD65/67 and anti-GlyT1 label large (>40% of syntaxin-1$^+$ amacrines) mutually exclusive populations of amacrine cells (Figure 2C and Table 2).

GABAergic (GAD65/67$^+$) and glycinergic (GlyT1$^+$) amacrine cells were born in overlapping but distinct waves (Figure 3). The genesis of GABAergic amacrines reached a peak around E14, while the genesis of glycinergic amacrines peaks around birth (Figure 3A). Overall, there is about a 3-day interval between the ages at which 50% of GAD65/67$^+$ and GlyT1$^+$ amacrines have become postmitotic (Figure 3B), and their genesis accounts for most if not the entire amacrine birthdating interval.

Distinct birthdays of GABAergic amacrine subsets

Glycinergic and GABAergic amacrine cells are both heterogeneous groups. Our observation that they are born at distinct times raised the question of whether there are only three waves in amacrine genesis, or whether these three waves can be subdivided further. To address this issue, we used additional markers to distinguish sub-subsets of amacrine cells. These included antibodies to neuropeptides (neuropeptide Y), neurotransmitter synthesizing enzymes (tyrosine hydroxylase and choline acetyltransferase [TH, ChAT]), neurotransmitter transporters (vesicular glutamate transporter 3 [VGlut3]), and transcription factors (Ebf) (Davis and Reed, 1996; Haverkamp and Wassle, 2000; 2004; Johnson et al., 2004; Menger et al., 1998). Examples are shown in Figure 4 and data are summarized in Table 2.

Cholinergic (ChAT$^+$) amacrines, also known as starburst amacrines, and NPY-containing amacrines both express GAD65/67 and are thus GABAergic, consistent with previous reports (Sinclair and Nirenberg, 2001; Vaney, 1990) (Figure 4B and data not shown). Double labeling for ChAT and NPY showed that the former are a subset of the latter: all ChAT$^+$ amacrines contain NPY protein (Figure 4A) and express NPY RNA (data not shown), but only ~66% of the NPY cells express ChAT. The NPY$^+$, ChAT$^-$ cells are likely to be a uniform subset since the vast majority project to the single inner plexiform sublayer S1 (Figure 4A; Sinclair and Nirenberg, 2001). The coincidence of these two markers was not noted previously, probably because the expression of NPY is developmentally regulated, as seen by comparing Figures 4A (which shows a P7 retina) and 4C (which shows a P14 retina). At P7, NPY levels are high

in starburst amacrine cell bodies and processes; its levels decrease in starburst processes but are retained by amacrine cell bodies and the processes in S1 at P14. By 3 months of age, NPY is barely detectable in any amacrines (data not shown).

We determined the birthdates of ChAT[+] and NPY[+] amacrines and compared them with those of GABAergic amacrines. Both ChAT[+] and NPY^{+} cells were generated at the beginning of the GABAergic wave (Figure 5A). Significant numbers of both populations (20–30%) were postmitotic at E10, when less than 5% of the GABAergic amacrines were born, and ~90% were postmitotic by E14 when only ~50% of GAD65/67[+] amacrines had been generated. (Figure 5B). Moreover, birthdates of ChAT[+] amacrines precede those of NPY[+] amacrines (Figure 5B). In that ChAT[+] amacrines are a subpopulation of the NPY[+] subset, NPY[+], ChAT[−] amacrines are born after the NPY[+], ChAT[+] amacrines. Likewise, NPY[−] GABAergic amacrines are presumably born after NPY[+] amacrines. Thus, we infer that three subsets of GABAergic amacrine cells have substantially different times of birth: first ChAT[+], NPY[+], GAD65/67[+], then ChAT[−], NPY[+], GAD65/67[+] followed by ChAT[−], NPY[−], GAD65/67[+] (Figure 5C). Finally, tyrosine hydroxylase (TH)-immunoreactive amacrines, which have been reported to be GABAergic in mice and other species (Haverkamp and Wassle, 2000; Wulle and Wagner, 1990), were born within the GAD65/67 wave, but later than the NPY[+] subset (Figure 5). Thus, much like the main retinal neuron types and like the large amacrine subtypes, sub-subtypes of GABAergic neurons appear to possess distinct birthdays.

We also asked whether subsets of the glycinergic amacrine cells are born at distinct times. This study was less conclusive because there are fewer known definitive markers for glycinergic amacrine subsets. The two markers we used, Vglut3 and pan-Ebf, do indeed label glycinergic subsets (Figure 4D–F); however each marker also labels some GlyT1-negative amacrines as well. Antibodies to Disabled-1, which marks the well-characterized glycinergic AII amacrines (Rice and Curran, 2000), did not label tissue that had been treated with HCl, as required by the BrdU staining protocol. We therefore calculated separately the birthdates of the innermost row of GlyT1+ cells, which presumably comprise the entire AII and part of the A8 populations of bilaminar glycinergic amacrines (Heinze et al., 2007; Pourcho and Goebel, 1985). Thus, although the birthdating curves of the AII plus A8, and Vglut3^{+} subsets precede that of the glycinergic amacrines generally (Figure 5D), it is unclear whether glycinergic amacrine subsets may share birthdays.

Centrifugal gradient of amacrine birthdates

Retinogenesis proceeds in a centrifugal manner: the birth of retinal neurons starts in the center and spreads radially, reaching the periphery with a delay of 2–3 days in rodents (Rapaport et al., 2004; Young, 1985a). We asked whether the center to periphery gradient of genesis is a general property of amacrines, or whether subsets differ in the spatial dynamics of their production. To this end, we compared the birthdates of the seven amacrine subsets described above in central retina (data in Figure 3 and 5) with birthdates in peripheral retina. For all eight types, cells in the periphery were born later than those in the center (Figure 6A). Moreover, the delay from center to periphery was similar for all subsets, so the sequence of birthdates in central retina was maintained in peripheral retina (Figure 6D).

Relationship of amacrine birthdates and soma position

In some parts of the vertebrate central nervous system, such as cerebral cortex, neuronal birthday in the ventricular zone is related to the soma position in the mature tissue (see Introduction). In retina, by contrast, such a relationship has not been obvious: ganglion cells and cones are both born early but end up at opposite poles within the retina; likewise, horizontal and amacrine cells are both born earlier than bipolars, which eventually lie between them (Young, 1985a). We asked whether subsets of amacrine cells might exhibit a more regular

relationship between their birthday and soma position than do the fundamentally different neuronal types.

Amacrine cells, in general, occupy the inner half of the inner nuclear layer and comprise 3–4 rows of cells (Figure 7A). There are also amacrines displaced to the ganglion cell layer (GCL). Immunostaining showed that somata of distinct amacrine subsets differ systematically in position (Figure 7B–D). For example, somata of ChAT$^+$ and NPY$^+$ amacrines are present in both the inner nuclear and the ganglion cell layers (as shown previously for ChAT$^+$ amacrines), whereas TH$^+$ and GlyT1$^+$ amacrines are confined to the inner nuclear layer. Within the inner nuclear layer, somata of most ChAT$^+$ and NPY$^+$ amacrines are adjacent to the inner plexiform layer, whereas Ebf$^+$ somata are closer to the outer plexiform layer (Figure 7E–K).

We tested the idea that the characteristic location of amacrine subtypes can be explained by their birthdates. If this hypothesis is true, then there should be a regular relationship between the time of cell cycle exit and laminar position within the inner nuclear layer and ganglion cell layer. To address this question, we calculated the mean position of BrdU$^+$, syntaxin-1$^+$ amacrine cells following injections at six time points (see Methods). This analysis revealed a strong linear relationship between position and birthdate ($r^2 = 0.91$), with the earliest-born amacrines tending to occupy the ganglion cell layer and innermost positions within the inner nuclear layer, while later-born cells were more distal (Figure 7L). Thus, as in cerebral cortex (Molyneaux et al., 2007), there is a systematic relationship between amacrine birthday and amacrine soma position, although the direction of the relationship differs between these two tissues (see Discussion).

We also analyzed our data on birthdates of amacrine subsets to ask whether the soma position of each subset was correlated with the subset's birthdate. Indeed, the time at which 50% of a given population became postmitotic (see Figure 6D) was strongly correlated with the final location of that subset's somata along the proximal-distal axis (Figure 7M; $r^2=0.86$).

As a final test of the idea that cell body position is correlated with birthdate, we took advantage of the fact that NPY$^+$ and ChAT$^+$ amacrines are present in both inner nuclear and ganglion cell layers. For both subtypes, the amacrines in the ganglion cell layer were born before those in the inner nuclear layer (Figure 7N,O). Together, these results demonstrate that amacrines are born in a basal-to-apical gradient, and as a result, later-born amacrine subsets reside more distally within the inner nuclear layer.

We also asked whether there is a relationship between the birthdates of amacrine subsets and the laminae in the inner plexiform layer where their processes arborize, but no obvious correlation could be established (data not shown).

Subset specification in dissociated retinal cultures

The observation that birthday is related to both soma position and subset identity raises the question of how these attributes are related to each other. On one hand, subset identity could be determined by factors that act as or soon after amacrines exit the cell cycle. In this case, birthday would affect identity and soma position independently. Alternatively, subset identity could be determined by factors that amacrines encounter at their destination. In this case, birth order could determine destination, perhaps by a passive "stacking" mechanism, and destination could in turn influence identity. To distinguish these possibilities, we labeled dividing cells with BrdU as above, but then dissociated them before they accumulated cell type-specific markers. We asked whether the relationship between birthday and subtype identity was maintained when all amacrines differentiated in a uniform setting, and all spatial information was lost.

We injected pregnant females with BrdU on embryonic days E14 or E17. The total number of amacrine cells generated at these two times is similar (Figure 1D), but the subtype frequency differs: more NPY[+] than GlyT1^{+} cells are born at E14, the opposite is true at E17, and similar numbers of GAD65/67[+] amacrines are born at both times (Figure 3 and 5). Retinas were dissociated at P0, before they expressed NPY or GlyT1 at detectable levels (data not shown). Cells were cultured for nine days, then immunolabeled for NPY, GlyT1 or GAD65/67 (Figure 8B–D). In each case, cells were also stained for syntaxin-1, the pan-amacrine marker, and for BrdU, to label cells exiting the cell cycle at E14 or E17. We then counted the percentages of BrdU-positive amacrine cells labeled with one of the subset-specific markers, and compared these values to those obtained in vivo.

Results are shown in Figure 8E–H. For NPY-expressing amacrines, if cells acquired their fate before P0, a larger fraction of NPY^{+} cells would be BrdU-positive when the label was delivered at E14 than when it was delivered at E17, based on results from in vivo studies. Alternatively, if these cells acquire their fate after P0, they would all receive the same information in vitro, so the fraction of NPY cells that are BrdU-positive would be similar whether BrdU was delivered on E14 or E17. In fact, many NPY^{+} cells were BrdU-positive when label was delivered at E14, but no NPY[+], BrdU[+] double-positive afmacrines were detected following delivery of label at E17, indicating that NPY cells are specified before P0. Conversely, in the same cultures more GlyT1^{+} cells were labeled by BrdU at E17 than at E14, consistent with their late birth in vivo and with the hypothesis that subset fate is specified before P0. We also stained for GABAergic cells, which are born in roughly equal numbers at E14 and E17; as expected, similar numbers of GAD65/67^{+} cells were BrdU-positive following labeling at E14 and E17. Thus, for all three populations assayed, the results in vitro match those in vivo: despite being deprived of spatial cues during the period they acquired subtype-specific features, amacrines born at each age made fate choices appropriate to their birthdays.

DISCUSSION

The many dozens of neuronal types that comprise the vertebrate nervous system – for example motoneurons in the spinal cord, Purkinje cells in the cerebellum or sensory neurons in dorsal root ganglia – are only the tip of a large iceberg: many major types can be subdivided into dozens of subtypes, distinguishable by position, structure and function. In only a few cases do we have any insight into how these subtypes diversify as they develop and these so far reveal little commonality. Morphogens with graded distributions along the dorsal-ventral and rostrocaudal axes of the spinal cord lead to allocation of motoneurons to distinct motor pools (Dalla Torre di Sanguinetto et al., 2008; Jessell, 2000); lateral interactions among retinal cells lead to specification of 8 distinct photoreceptor types in the Drosophila ommatidium (Voas and Rebay, 2004); and differences in birthdate lead to laminar distinctions among cortical projection neurons (Molyneaux et al., 2007). Here, we addressed this issue with respect to retinal amacrine cells. Our results suggest that amacrine subsets are specified in ways related to those that govern cortical neuronal identity.

Relationship of amacrine birthday to subtype identity

Amacrine cells are inhibitory interneurons that receive and form synapses in the inner plexiform layer; they shape visual responses by mediating interactions among bipolar, retinal ganglion and other amacrine cells. Although all amacrines share these features, morphological studies have revealed the existence of over 30 amacrine subtypes in mammalian retinas, distinguished in large part by the diameter and laminar restriction of their arbor in the inner plexiform layer (MacNeil et al., 1999; MacNeil and Masland, 1998; Masland, 2001; Schubert et al., 2008; Wassle et al., 1998). Several subtypes can also be distinguished molecularly, particularly by differential expression of neurotransmitter synthetic enzymes, neurotransmitter

transporters, neuropeptides and calcium binding proteins (Haverkamp and Wassle, 2000; Vaney, 1990).

For reasons detailed in the Introduction, we favored the possibility that amacrines of different types might be specified by factors acting at or soon after the time their unspecified progenitors become post-mitotic. For this scheme to be valid, different amacrine subtypes would need to be born during distinct intervals. To test this idea, we began with the conventional subdivision of amacrines into GABAergic and glycinergic groups. In general, GABAergic amacrines in mammalian retinas have large broad dendritic arbors, suited to mediate lateral interaction, whereas glycinergic amacrines have narrow arbors that span multiple inner plexiform sublaminae and appear to mediate interlaminar interactions (Vaney, 1990). We found that GABAergic amacrines are born significantly prior to glycinergic amacrines (Figure 3). It is interesting to speculate that the early origin of wide-field amacrines, when the inner plexiform layer is relatively uncomplicated, may facilitate expansion of their arbors.

We next asked whether times of origin could be subdivided further within these broad classes. This was feasible for GABAergic cells, because $ChAT^+$ and NPY^+ cells are subsets of the GABAergic population (Brecha et al., 1988; Kosaka et al., 1988; Sinclair and Nirenberg, 2001; Vaney and Young, 1988). Indeed, $ChAT^+$ starburst amacrines form a subset of the NPY^+ population; this coexpression was not appreciated previously, probably because levels of NPY decrease in starbursts as they mature. In fact, $ChAT^+$, NPY^+, GAD^+ amacrines, $ChAT^-$, NPY^+, GAD^+ amacrines, and $ChAT^-$, NPY^-, GAD^+ amacrines are born at different times (Figure 5). Thus, amacrine subsets – including sub-subsets of the GABAergic class – have distinct yet overlapping birthdates. These results suggest that mechanisms operating within progenitors to diversify amacrines may be similar to the mechanisms that generate diversity at the main cell type level (Livesey and Cepko, 2001). Available markers did not allow us to obtain clear-cut results for subsets of glycinergic amacrines.

Our results are broadly consistent with those of studies that have determined birthdates of amacrine subsets in rats, including dopaminergic (Evans and Battelle, 1987), substance P- and corticotropin releasing factor-like immunoreactive (Zhang and Yeh, 1992; Zhang and Yeh, 1990), ChAT-positive (Reese and Colello, 1992), and GABA-positive amacrines (Lee et al., 1999). In no previous case, however, were birthdates of subsets compared to each other or to amacrines generally. Thus, our study is the first to analyze the relative order of birthdates for amacrine subsets.

Relationship of amacrine birthday to soma position

We asked whether amacrine birthdate varies systematically with retinal position. The center to periphery gradient observed for the main retinal cell types (Hu and Easter, 1999; Young, 1984) also applies to subsets of amacrine cells. Moreover, the sequence in the production of different subtypes is similar in central and peripheral retina (Figure 6). More interesting was an unexpected relationship of birthday to soma position along the apical-basal axis (Figure 7). This relationship was apparent by three measures. First, the location of $BrdU^+$ amacrine cells within the inner nuclear layer was correlated with their birthdate. Second, the mean birthdate of each subset was correlated with the mean position of its somata. Third, within the $ChAT^+$ and NPY^+ subsets, displaced amacrines in the ganglion cell layer were born before those in the inner nuclear layer (see also (Lee et al., 1999)). Together, these results reveal a systematic relationship between the time at which an amacrine cell is born and the position to which it eventually migrates.

The relationship between birthday and soma position in retina is reminiscent of that documented for projection neurons in cerebral cortex (Leone et al., 2008; McConnell, 1985; Metin et al., 2006; Molyneaux et al., 2007; Shen et al., 2006). A striking difference is that

cortical neurons settle in an inside-out, apical-to-basal order, with each successive wave migrating past its predecessors, whereas amacrine cells settle in an outside-in, basal-to-apical order. Thus, in contrast to the complex migratory guidance systems needed to target cortical neurons to proper layers (Metin et al., 2006), a simple passive stacking mechanism might account for the relationship of birth order to soma position for amacrines.

Relationships of amacrine soma position to subtype identity

The existence of a systematic relationship between soma position and subtype identity raised the question of whether subtype identity is determined by influences acting on newborn neurons, or whether neurons migrate to appropriate destinations and then encounter spatially deployed extrinsic factors that determine their identity. For cortex, this question was answered by elegant transplantation experiments, which showed that neurons have acquired the information needed to migrate to appropriate layers and acquire subtype-specific properties by the time they complete their final mitosis (Leone et al., 2008; McConnell, 1985). Such transplantation experiments are infeasible in retina, so instead we asked whether the relationship between birthdate and subtype identity would be manifest when amacrines were dissociated and cultured in a uniform environment soon after they were born and before they had acquired subtype-specific markers.

In fact, relative birth orders for three subtypes (NPY-positive, GABAergic and glycinergic) were preserved under these conditions (Figure 8). It is likely that some NPY-positive cells had migrated to the nascent inner nuclear layer before dissociation, so we cannot exclude the possibility that local cues triggered a program of differentiation that was then executed in vitro. In contrast, many GABAergic and most glycinergic amacrines reach their destinations only postnatally. Indeed, it is likely that few cells labeled by BrdU at E17 had reached their destination by P0. Thus, for glycinergic cells, our results provide strong evidence that subtype identity is acquired prior to reaching their destination and quite possibly while they (or their progenitors) still reside in the neuroblast layer.

Together, our results are consistent with those reached for the main retinal types and for cortical pyramidal cells. In each case, neuroblasts express a repertoire of transcription factors that changes over time and restricts the competence of progenitor cells to a few cell fates within a certain time frame (Cayouette et al., 2006; Cepko et al., 1996; Leone et al., 2008; Livesey and Cepko, 2001; Metin et al., 2006; Molyneaux et al., 2007). Extrinsic signals then specify cell fate within the range to which the progenitor is restricted. Likewise, the sequential generation of amacrine subsets, and their birthdate-appropriate differentiation *in vitro* suggest that a similar model applies to them. The accessibility of the retina and the growing set of molecular labels available for amacrine subsets recommend this system for elucidation of principles that may be applicable to the less accessible cortex.

Acknowledgments

REFERENCE

Alexiades MR, Cepko C. Quantitative analysis of proliferation and cell cycle length during development of the rat retina. Dev Dyn 1996;205(3):293–307. [PubMed: 8850565]

Barnstable CJ, Hofstein R, Akagawa K. A marker of early amacrine cell development in rat retina. Brain Res 1985;352(2):286–290. [PubMed: 3896407]

Brecha N, Johnson D, Peichl L, Wassle H. Cholinergic amacrine cells of the rabbit retina contain glutamate decarboxylase and gamma-aminobutyrate immunoreactivity. Proc Natl Acad Sci U S A 1988;85(16):6187–6191. [PubMed: 3413087]

Brody T, Odenwald WF. Cellular diversity in the developing nervous system: a temporal view from Drosophila. Development 2002;129(16):3763–3770. [PubMed: 12135915]

Brunelli G, Spano P, Barlati S, Guarneri B, Barbon A, Bresciani R, Pizzi M. Glutamatergic reinnervation through peripheral nerve graft dictates assembly of glutamatergic synapses at rat skeletal muscle. Proc Natl Acad Sci U S A 2005;102(24):8752–8757. [PubMed: 15937120]

Burmeister M, Novak J, Liang MY, Basu S, Ploder L, Hawes NL, Vidgen D, Hoover F, Goldman D, Kalnins VI, Roderick TH, Taylor BA, Hankin MH, McInnes RR. Ocular retardation mouse caused by Chx10 homeobox null allele: impaired retinal progenitor proliferation and bipolar cell differentiation. Nat Genet 1996;12(4):376–384. [PubMed: 8630490]

Cayouette M, Barres BA, Raff M. Importance of intrinsic mechanisms in cell fate decisions in the developing rat retina. Neuron 2003;40(5):897–904. [PubMed: 14659089]

Cayouette M, Poggi L, Harris WA. Lineage in the vertebrate retina. Trends Neurosci 2006;29(10):563–570. [PubMed: 16920202]

Cepko CL, Austin CP, Yang X, Alexiades M, Ezzeddine D. Cell fate determination in the vertebrate retina. Proc Natl Acad Sci U S A 1996;93(2):589–595. [PubMed: 8570600]

Dalla Torre di Sanguinetto SA, Dasen JS, Arber S. Transcriptional mechanisms controlling motor neuron diversity and connectivity. Curr Opin Neurobiol 2008;18(1):36–43. [PubMed: 18524570]

Davis JA, Reed RR. Role of Olf-1 and Pax-6 transcription factors in neurodevelopment. J Neurosci 1996;16(16):5082–5094. [PubMed: 8756438]

Edlund T, Jessell TM. Progression from extrinsic to intrinsic signaling in cell fate specification: a view from the nervous system. Cell 1999;96(2):211–224. [PubMed: 9988216]

Elshatory Y, Deng M, Xie X, Gan L. Expression of the LIM-homeodomain protein Isl1 in the developing and mature mouse retina. J Comp Neurol 2007;503(1):182–197. [PubMed: 17480014]

Evans JA, Battelle BA. Histogenesis of dopamine-containing neurons in the rat retina. Exp Eye Res 1987;44(3):407–414. [PubMed: 3595756]

Fremeau RT Jr. Burman J, Qureshi T, Tran CH, Proctor J, Johnson J, Zhang H, Sulzer D, Copenhagen DR, Storm-Mathisen J, Reimer RJ, Chaudhry FA, Edwards RH. The identification of vesicular glutamate transporter 3 suggests novel modes of signaling by glutamate. Proc Natl Acad Sci U S A 2002;99(22):14488–14493. [PubMed: 12388773]

Gerrero MR, McEvilly RJ, Turner E, Lin CR, O'Connell S, Jenne KJ, Hobbs MV, Rosenfeld MG. Brn-3.0: a POU-domain protein expressed in the sensory, immune, and endocrine systems that functions on elements distinct from known octamer motifs. Proc Natl Acad Sci U S A 1993;90(22):10841–10845. [PubMed: 8248179]

Gras C, Herzog E, Bellenchi GC, Bernard V, Ravassard P, Pohl M, Gasnier B, Giros B, El Mestikawy S. A third vesicular glutamate transporter expressed by cholinergic and serotoninergic neurons. J Neurosci 2002;22(13):5442–5451. [PubMed: 12097496]

Guillery RW. On counting and counting errors. J Comp Neurol 2002;447(1):1–7. [PubMed: 11967890]

Gurdon JB, Bourillot PY. Morphogen gradient interpretation. Nature 2001;413(6858):797–803. [PubMed: 11677596]

Harman AM, Beazley LD. Generation of retinal cells in the wallaby, Setonix brachyurus (quokka). Neuroscience 1989;28(1):219–232. [PubMed: 2761691]

Haverkamp S, Wassle H. Immunocytochemical analysis of the mouse retina. J Comp Neurol 2000;424 (1):1–23. [PubMed: 10888735]

Haverkamp S, Wassle H. Characterization of an amacrine cell type of the mammalian retina immunoreactive for vesicular glutamate transporter 3. J Comp Neurol 2004;468(2):251–263. [PubMed: 14648683]

Heinze L, Harvey RJ, Haverkamp S, Wassle H. Diversity of glycine receptors in the mouse retina: localization of the alpha4 subunit. J Comp Neurol 2007;500(4):693–707. [PubMed: 17154252]

Holt CE, Bertsch TW, Ellis HM, Harris WA. Cellular determination in the Xenopus retina is independent of lineage and birth date. Neuron 1988;1(1):15–26. [PubMed: 3272153]

Hu M, Easter SS. Retinal neurogenesis: the formation of the initial central patch of postmitotic cells. Dev Biol 1999;207(2):309–321. [PubMed: 10068465]

Inoue A, Akagawa K. Neuron specific expression of a membrane protein, HPC-1: tissue distribution, and cellular and subcellular localization of immunoreactivity and mRNA. Brain Res Mol Brain Res 1993;19(1–2):121–128. [PubMed: 8361334]

Inoue A, Obata K, Akagawa K. Cloning and sequence analysis of cDNA for a neuronal cell membrane antigen, HPC-1. J Biol Chem 1992;267(15):10613–10619. [PubMed: 1587842]

Jeon CJ, Strettoi E, Masland RH. The major cell populations of the mouse retina. J Neurosci 1998;18 (21):8936–8946. [PubMed: 9786999]

Jessell TM. Neuronal specification in the spinal cord: inductive signals and transcriptional codes. Nat Rev Genet 2000;1(1):20–29. [PubMed: 11262869]

Johnson J, Sherry DM, Liu X, Fremeau RT Jr. Seal RP, Edwards RH, Copenhagen DR. Vesicular glutamate transporter 3 expression identifies glutamatergic amacrine cells in the rodent retina. J Comp Neurol 2004;477(4):386–398. [PubMed: 15329888]

Kahn AJ. An autoradiographic analysis of the time of appearance of neurons in the developing chick neural retina. Dev Biol 1974;38(1):30–40. [PubMed: 4856982]

Kitabatake Y, Hikida T, Watanabe D, Pastan I, Nakanishi S. Impairment of reward-related learning by cholinergic cell ablation in the striatum. Proc Natl Acad Sci U S A 2003;100(13):7965–7970. [PubMed: 12802017]

Kosaka T, Tauchi M, Dahl JL. Cholinergic neurons containing GABA-like and/or glutamic acid decarboxylase-like immunoreactivities in various brain regions of the rat. Exp Brain Res 1988;70 (3):605–617. [PubMed: 3384059]

La Vail MM, Rapaport DH, Rakic P. Cytogenesis in the monkey retina. J Comp Neurol 1991;309(1):86–114. [PubMed: 1894769]

Lee MY, Shin SL, Han SH, Chun MH. The birthdates of GABA-immunoreactive amacrine cells in the rat retina. Exp Brain Res 1999;128(3):309–314. [PubMed: 10501803]

Lefebvre JL, Zhang Y, Meister M, Wang X, Sanes JR. gamma-Protocadherins regulate neuronal survival but are dispensable for circuit formation in retina. Development 2008;135(24):4141–4151. [PubMed: 19029044]

Leone DP, Srinivasan K, Chen B, Alcamo E, McConnell SK. The determination of projection neuron identity in the developing cerebral cortex. Curr Opin Neurobiol 2008;18(1):28–35. [PubMed: 18508260]

Li S, Mo Z, Yang X, Price SM, Shen MM, Xiang M. Foxn4 controls the genesis of amacrine and horizontal cells by retinal progenitors. Neuron 2004;43(6):795–807. [PubMed: 15363391]

Liu IS, Chen JD, Ploder L, Vidgen D, van der Kooy D, Kalnins VI, McInnes RR. Developmental expression of a novel murine homeobox gene (Chx10): evidence for roles in determination of the neuroretina and inner nuclear layer. Neuron 1994;13(2):377–393. [PubMed: 7914735]

Livesey FJ, Cepko CL. Vertebrate neural cell-fate determination: lessons from the retina. Nat Rev Neurosci 2001;2(2):109–118. [PubMed: 11252990]

MacNeil MA, Heussy JK, Dacheux RF, Raviola E, Masland RH. The shapes and numbers of amacrine cells: matching of photofilled with Golgi-stained cells in the rabbit retina and comparison with other mammalian species. J Comp Neurol 1999;413(2):305–326. [PubMed: 10524341]

MacNeil MA, Masland RH. Extreme diversity among amacrine cells: implications for function. Neuron 1998;20(5):971–982. [PubMed: 9620701]

Masland RH. Neuronal diversity in the retina. Curr Opin Neurobiol 2001;11(4):431–436. [PubMed: 11502388]

McConnell SK. Migration and differentiation of cerebral cortical neurons after transplantation into the brains of ferrets. Science 1985;229(4719):1268–1271. [PubMed: 4035355]

Menger N, Pow DV, Wassle H. Glycinergic amacrine cells of the rat retina. J Comp Neurol 1998;401 (1):34–46. [PubMed: 9802699]

Metin C, Baudoin JP, Rakic S, Parnavelas JG. Cell and molecular mechanisms involved in the migration of cortical interneurons. Eur J Neurosci 2006;23(4):894–900. [PubMed: 16519654]

Molyneaux BJ, Arlotta P, Menezes JR, Macklis JD. Neuronal subtype specification in the cerebral cortex. Nat Rev Neurosci 2007;8(6):427–437. [PubMed: 17514196]

Packard DS Jr. Menzies RA, Skalko RG. Incorportaiton of thymidine and its analogue, bromodeoxyuridine, into embryos and maternal tissues of the mouse. Differentiation 1973;1(6):397–404. [PubMed: 4802502]

Pequignot MO, Provost AC, Salle S, Taupin P, Sainton KM, Marchant D, Martinou JC, Ameisen JC, Jais JP, Abitbol M. Major role of BAX in apoptosis during retinal development and in establishment of a functional postnatal retina. Dev Dyn 2003;228(2):231–238. [PubMed: 14517994]

Pourcho RG, Goebel DJ. A combined Golgi and autoradiographic study of (3H)glycine-accumulating amacrine cells in the cat retina. J Comp Neurol 1985;233(4):473–480. [PubMed: 2984258]

Rapaport DH, Wong LL, Wood ED, Yasumura D, LaVail MM. Timing and topography of cell genesis in the rat retina. J Comp Neurol 2004;474(2):304–324. [PubMed: 15164429]

Reese BE, Colello RJ. Neurogenesis in the retinal ganglion cell layer of the rat. Neuroscience 1992;46 (2):419–429. [PubMed: 1542415]

Rice DS, Curran T. Disabled-1 is expressed in type AII amacrine cells in the mouse retina. J Comp Neurol 2000;424(2):327–338. [PubMed: 10906706]

Schafer MK, Varoqui H, Defamie N, Weihe E, Erickson JD. Molecular cloning and functional identification of mouse vesicular glutamate transporter 3 and its expression in subsets of novel excitatory neurons. J Biol Chem 2002;277(52):50734–50748. [PubMed: 12384506]

Schubert T, Kerschensteiner D, Eggers ED, Misgeld T, Kerschensteiner M, Lichtman JW, Lukasiewicz PD, Wong RO. Development of presynaptic inhibition onto retinal bipolar cell axon terminals is subclass-specific. J Neurophysiol 2008;100(1):304–316. [PubMed: 18436633]

Shen Q, Wang Y, Dimos JT, Fasano CA, Phoenix TN, Lemischka IR, Ivanova NB, Stifani S, Morrisey EE, Temple S. The timing of cortical neurogenesis is encoded within lineages of individual progenitor cells. Nat Neurosci 2006;9(6):743–751. [PubMed: 16680166]

Sidman, RL. Histogenesis of mouse retina studied with thymidine-H3. In: Smelser, GK., editor. The Structure of the Eye. 1961. p. 487-506.

Sinclair JR, Nirenberg S. Characterization of neuropeptide Y-expressing cells in the mouse retina using immunohistochemical and transgenic techniques. J Comp Neurol 2001;432(3):296–306. [PubMed: 11246209]

Ste Marie L, Luquet S, Cole TB, Palmiter RD. Modulation of neuropeptide Y expression in adult mice does not affect feeding. Proc Natl Acad Sci U S A 2005;102(51):18632–18637. [PubMed: 16339312]

Strettoi E, Masland RH. The number of unidentified amacrine cells in the mammalian retina. Proc Natl Acad Sci U S A 1996;93(25):14906–14911. [PubMed: 8962154]

Vaney DI. The mosaic of amacrine cells in the mammalian retina. Progress in retinal research 1990;9:49–100.

Vaney DI, Young HM. GABA-like immunoreactivity in cholinergic amacrine cells of the rabbit retina. Brain Res 1988;438(1–2):369–373. [PubMed: 3345446]

Voas MG, Rebay I. Signal integration during development: insights from the Drosophila eye. Dev Dyn 2004;229(1):162–175. [PubMed: 14699588]

Wassle H, Koulen P, Brandstatter JH, Fletcher EL, Becker CM. Glycine and GABA receptors in the mammalian retina. Vision Res 1998;38(10):1411–1430. [PubMed: 9667008]

Wulle I, Wagner HJ. GABA and tyrosine hydroxylase immunocytochemistry reveal different patterns of colocalization in retinal neurons of various vertebrates. J Comp Neurol 1990;296(1):173–178. [PubMed: 1972711]

Xiang M, Zhou L, Macke JP, Yoshioka T, Hendry SH, Eddy RL, Shows TB, Nathans J. The Brn-3 family of POU-domain factors: primary structure, binding specificity, and expression in subsets of retinal ganglion cells and somatosensory neurons. J Neurosci 1995;15(7 Pt 1):4762–4785. [PubMed: 7623109]

Young RW. Cell death during differentiation of the retina in the mouse. J Comp Neurol 1984;229(3):362–373. [PubMed: 6501608]

Young RW. Cell differentiation in the retina of the mouse. Anat Rec 1985a;212(2):199–205. [PubMed: 3842042]

Young RW. Cell proliferation during postnatal development of the retina in the mouse. Brain Res 1985b; 353(2):229–239. [PubMed: 4041905]

Zhang D, Yeh HH. Substance-P-like immunoreactive amacrine cells in the adult and the developing rat retina. Brain Res Dev Brain Res 1992;68(1):55–65.

Zhang DR, Yeh HH. Histogenesis of corticotropin releasing factor-like immunoreactive amacrine cells in the rat retina. Brain Res Dev Brain Res 1990;53(2):194–199.

Zimmerman RP, Polley EH, Fortney RL. Cell birthdays and rate of differentiation of ganglion and horizontal cells of the developing cat's retina. J Comp Neurol 1988;274(1):77–90. [PubMed: 3417908]
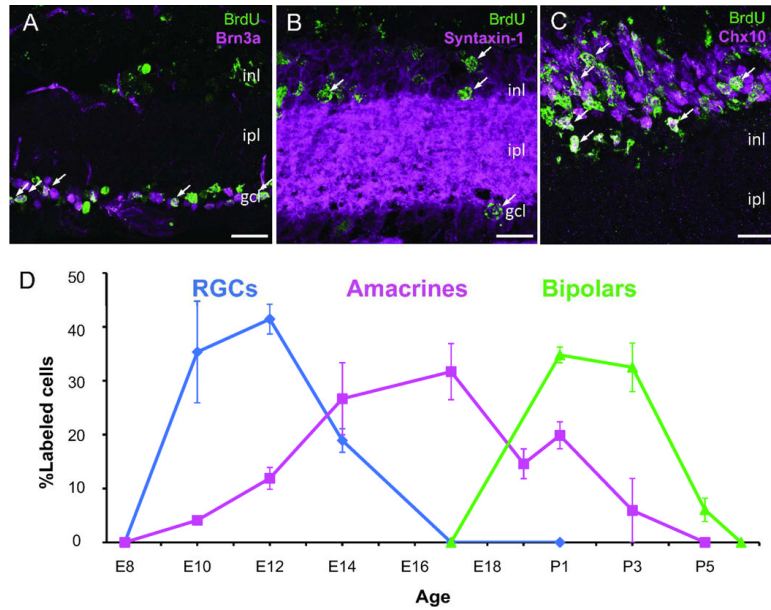
Figure 1. Birthdates of retinal neuron populations measured using BrdU
(A–C) Sections from P14–P15 retinas of animals injected with BrdU at E12 (A), E17 (B), or
P3 (C) to mark neurons that exited the cell cycle shortly after injection. Sections were double
labeled with markers for RGCs (Brn3a), amacrine cells (Syntaxin-1), or bipolar cells (Chx10)
as indicated. The predominant neuronal populations labeled with BrdU are RGCs at E12 (A),
amacrines at E17 (B), and bipolar cells at P3 (C), as shown by the double labeled cells (arrows).
Scale bar is 20μm. (D) Percentages of BrdU-labeled cells for each of three main retinal cell
populations. Amacrine cells are generated over a more protracted interval than retinal ganglion
or bipolar cells.
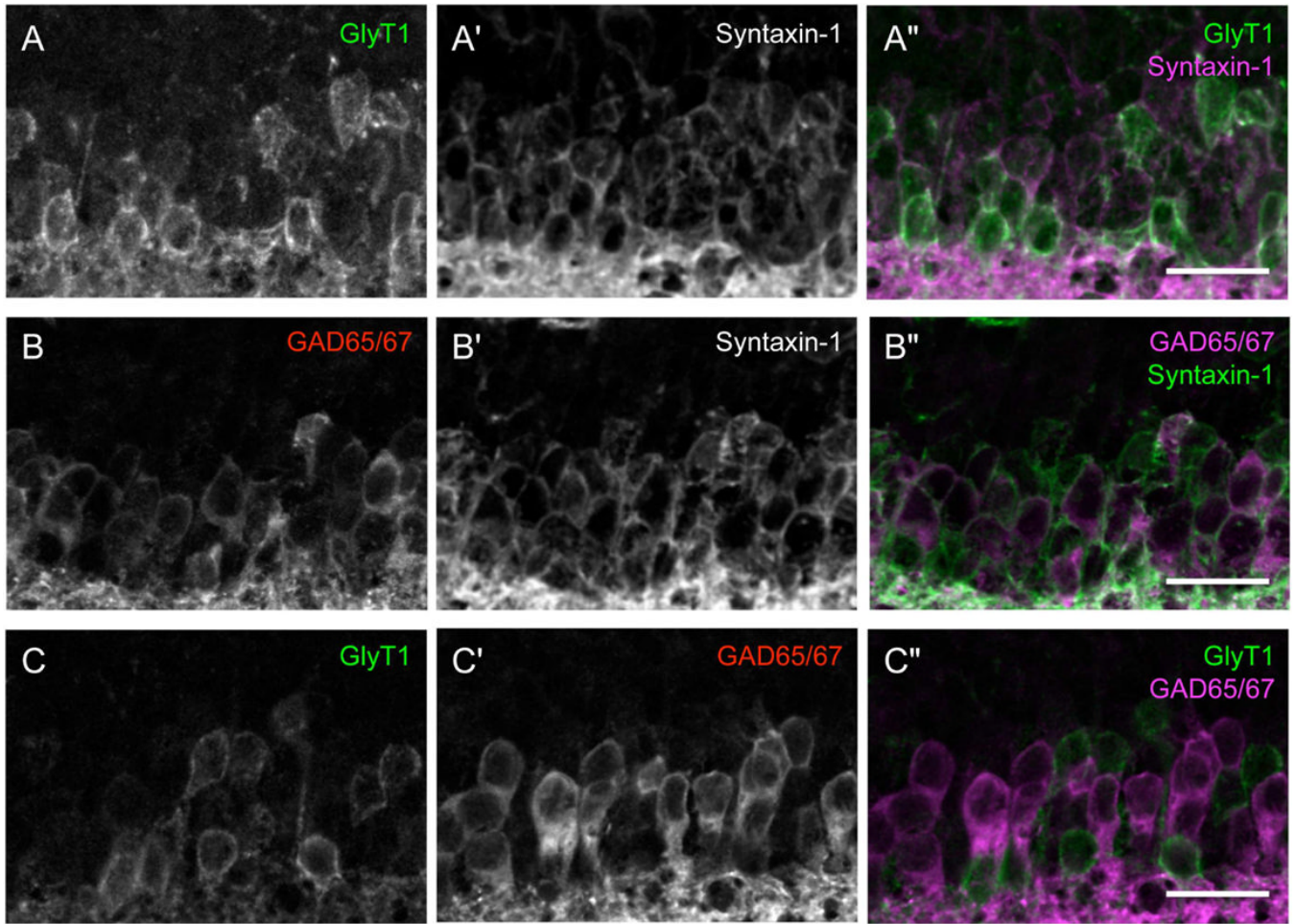
Figure 2. Subsets of amacrine cells defined by expression of GABAergic and glycinergic markers
Retinas from P15 mice, colabeled with antibodies against syntaxin-1, a pan-amacrine marker, and (A–A") GlyT1 or (B–B") GAD65/67, to label the major amacrine subsets. Both GAD65/67 and GlyT1 label a large number of cells, all of which express syntaxin-1. (C–C") Double label with GAD65/67 and GlyT1 reveals that the two amacrine cell populations are non-overlapping. Scale bar is 20μm.
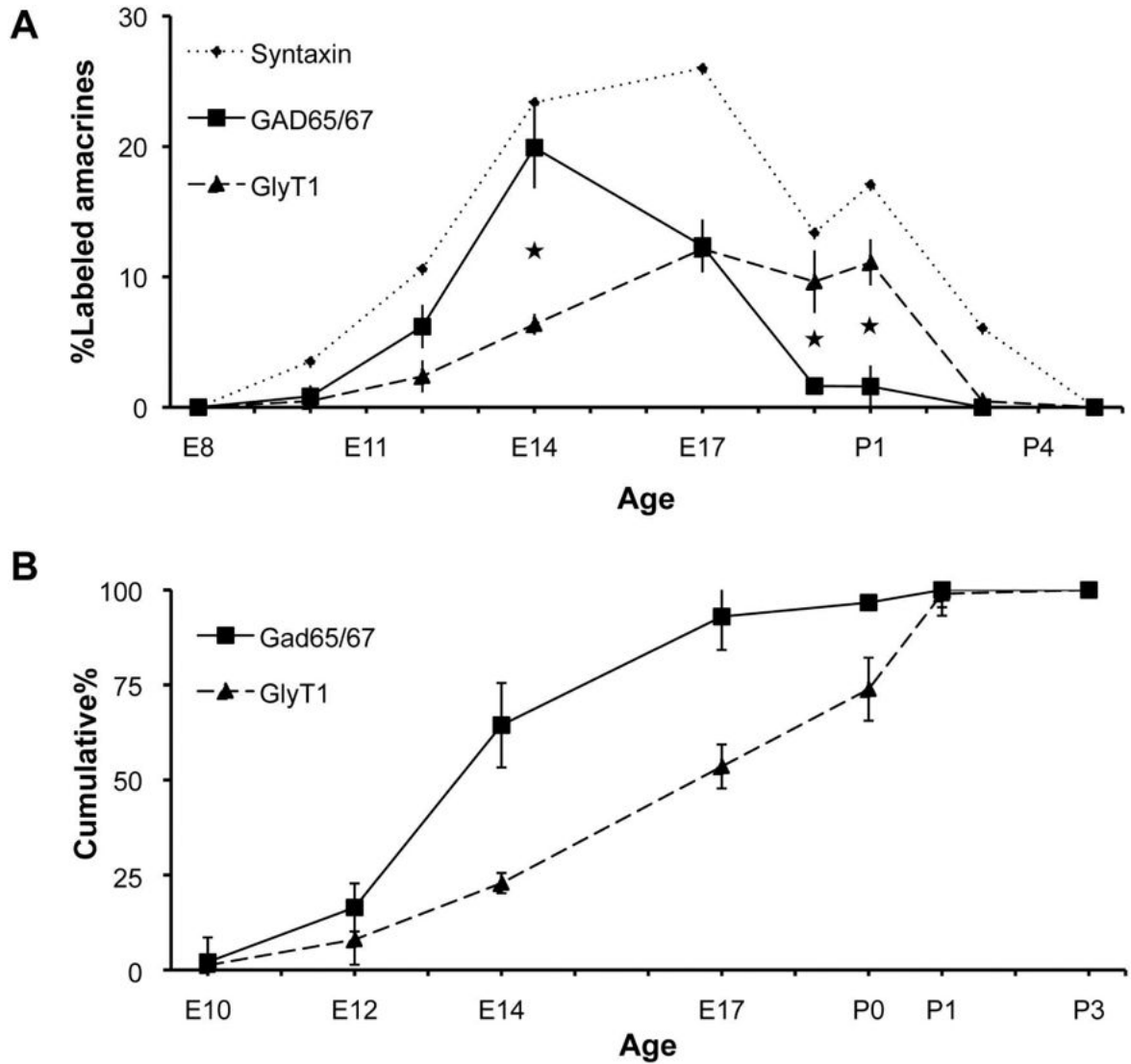
Figure 3. GABAergic amacrines are born before glycinergic amacrines
(A) Birthdate curves for GABAergic (GAD65/67[+]) and glycinergic (GlyT1^{+}) amacrines demonstrate that the two groups exit the cell cycle at different times. Data are presented as the percentage of the total amacrine population (labeled by syntaxin-1) that was double positive for BrdU and the given subset marker. Bars indicate ± SEM. Significant differences between GAD65/67[+] and GlyT1^{+} ($p < 0.05$) are shown by asterisks. (B) Cumulative birthdate curves, showing the fraction of each amacrine population born by a given age, emphasize the sequential birth of these two amacrine subsets. The cumulative percentage of BrdU-labeled cells within individual subset populations was calculated from data shown in (A). Bars indicate 90% confidence intervals.
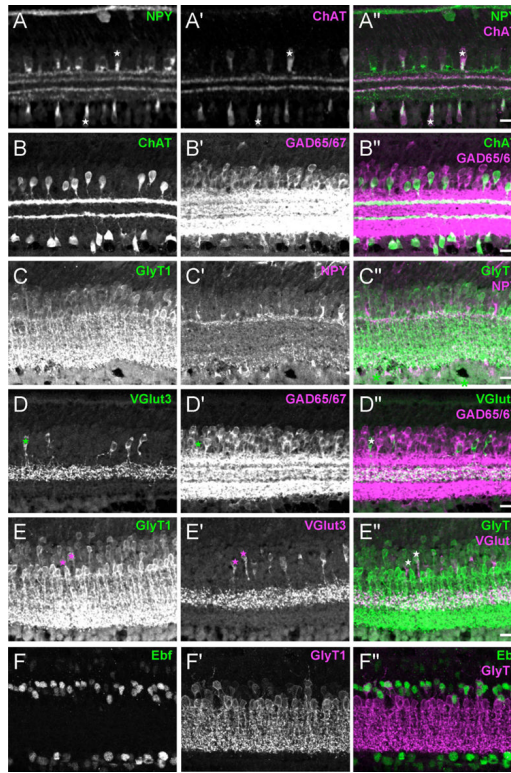
Figure 4. GABAergic and glycinergic amacrines are heterogeneous populations
Confocal images of retinas labeled with antibodies that mark amacrine subtypes. (A) ChAT$^+$ amacrines are a subset of NPY$^+$ amacrines; example of ChAT$^+$, NPY$^+$ cells (*). (B) ChAT$^+$ amacrines are a subset of the GAD65/67$^+$ amacrines. (C) Antibodies to GlyT1, NPY and TH label three non-overlapping populations (only channels for GlyT1 and NPY are shown separately). (D–E) Most VGlut3$^+$ amacrines express GlyT1 and none express GAD65/67. Asterisk in D' marks location of a VGlut3$^+$GAD65/67$^-$ amacrine cell; asterisks in E' mark examples of VGlut3$^+$GlyT1$^+$ amacrines. (F) Partial overlap between Ebf and GlyT1 amacrine cells. Retinas were from P7 (A) or P14–P15 (B–E) mice. Scale bar is 20μm.
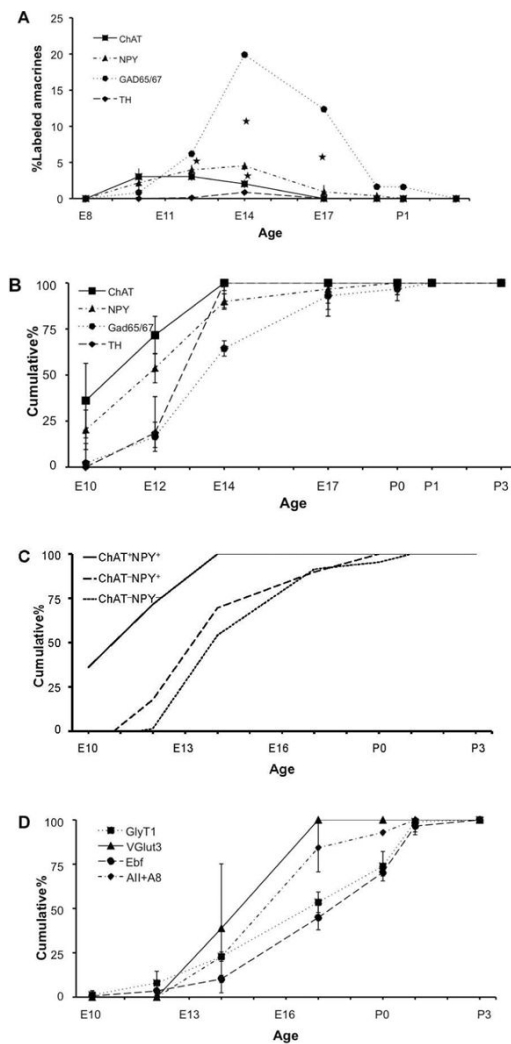
Figure 5. Birthdates of GABAergic and glycinergic amacrine subtypes
(A) Birthdate curves for GABAergic (GAD65/67[+]) amacrines and their cholinergic (ChAT[+]), neuropeptidergic (NPY[+]) and dopaminergic (TH[+]) subtypes. Data are presented as the percentage of the total amacrine population (labeled by syntaxin-1) that was double positive for BrdU and the given subset marker. Bars indicate ±SEM. Significant differences between GAD65/67[+], ChAT[+] and NPY[+] ($p < 0.05$) are shown by asterisks. (B–C) Cumulative birthdate curves reveal sequential generation of GABAergic amacrine subsets. The fraction of each amacrine population born by a given age, calculated from the data in (A) is plotted in (B) as the cumulative percentage of BrdU-labeled cells within individual subset populations. From these data, cumulative curves were calculated for three non-overlapping GABAergic subsets (C). (D) Cumulative birthdating curves for three subsets of amacrine cells that are largely glycinergic: Ebf[+], VGlut3^{+} and the AII and A8 amacrine cells. Bars indicate 90% confidence intervals.
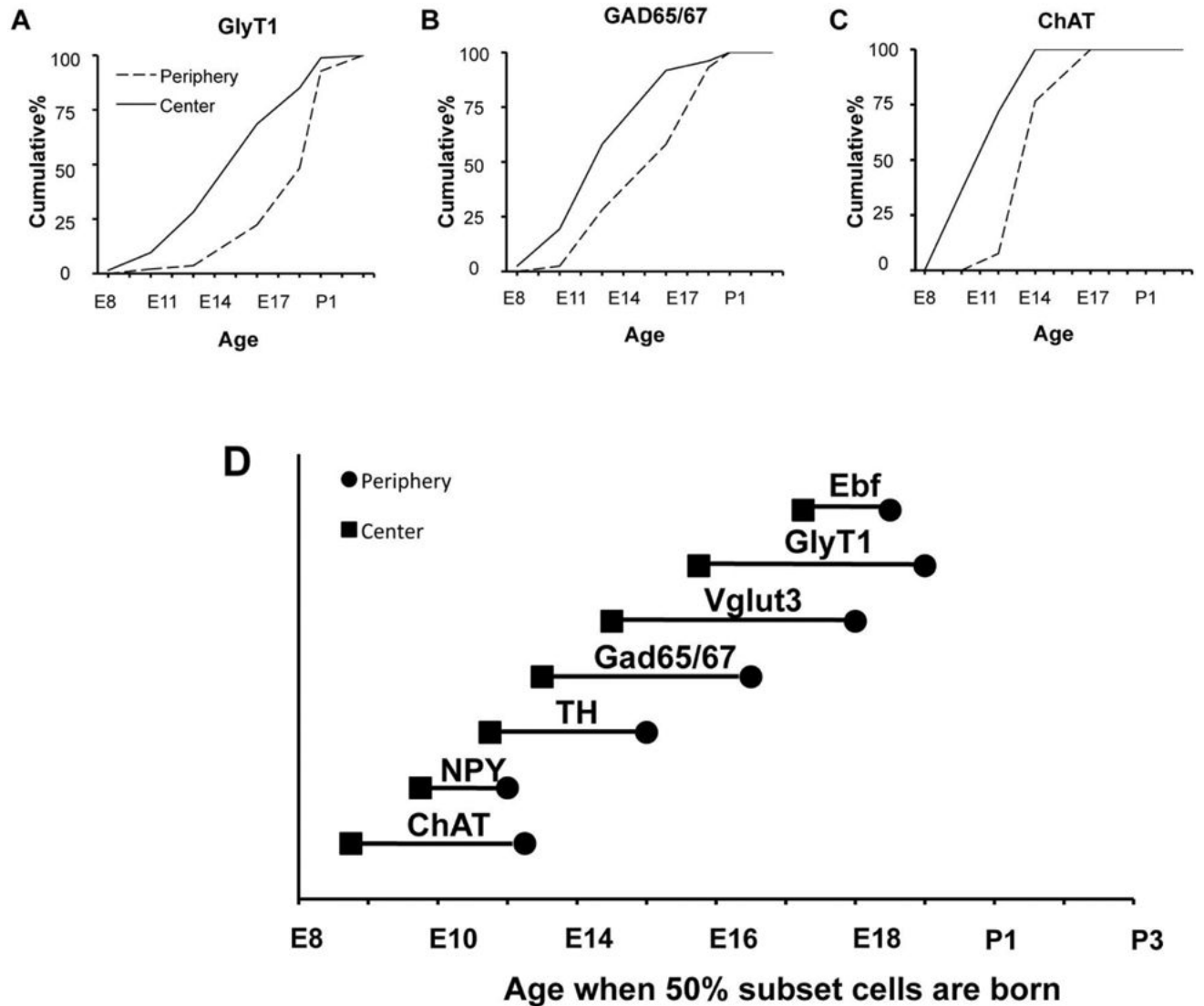
Figure 6. Amacrine subsets are born later in periphery than in central retina

(A–C) Cumulative birthdating curves in center and periphery for GlyT1+ (A), Gad 65/67+ (B), and ChAT+ (C) amacrines. Graphs show the cumulative percentage of cells born by a given age. (D) Birth order in peripheral and central retina, calculated from curves such as those in A–C. Data for central retina is replotted from Figures 3 and 5. Horizontal lines connect the 50% birthdate point for central and peripheral retina for each subset.
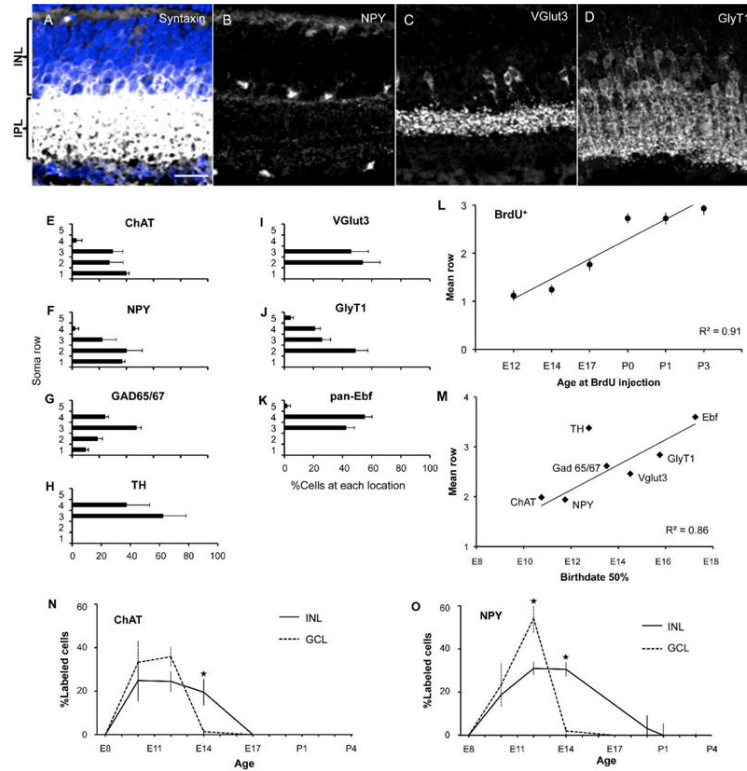
Figure 7. Correlation between soma position and birthdate

(A–D) Individual amacrine cell subsets have a consistent location within the INL (blue nuclear counterstain in A). (A) shows the pan-amacrine label, syntaxin-1, occupying about half of the INL. (B–D) show the location of three amacrine subsets. NPY^{+} cells reside in the INL close to the IPL and some are displaced in the GCL; VGlut3^{+} amacrines have a median position within the IPL part occupied by amacrine cells; and GlyT1^{+} amacrines are broadly distributed within the INL, reaching farther toward the outer retina than the other subsets. Scale bar is 20μm. (E) Graphs quantifying the distribution of amacrine subsets across 5 rows of cells. Row 1 corresponds to the ganglion cell layer, and 2 to 5 are nuclear rows of the INL, with 2 being the closest and 5 the farthest from the IPL. (F) Location of BrdU^{+} amacrines cells in the retina, following injections at six times. The earliest-born amacrines tend to occupy the ganglion cell layer and innermost positions within the INL, while later-born cells are successively more distal. Correlation between position and birthdate (r^2) is 0.91. (G) Scatter plot relating the 50% birthdate of each subset to the corresponding mean row in the retina, indicating that earlier-born subtypes have a more inner position. Each subset was represented proportional to its population size. (H) Birthdate curves for ChAT and NPY, showing that within a single subtype, displaced amacrines in the ganglion cell layer (dotted lines) are born before those in the INL (continuous lines)
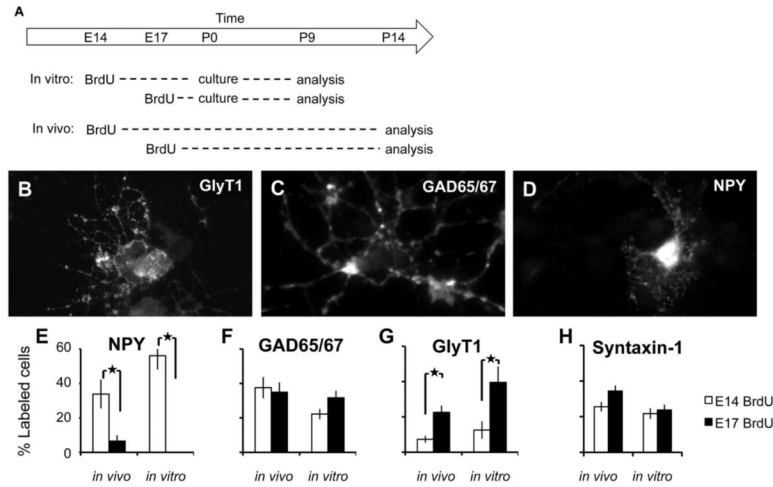
Figure 8. Amacrine subtype differentiation *in vitro*
(A) Experimental plan. Animals were injected with BrdU at embryonic days E14 or E17, then retinas were either sectioned and stained at P14 or dissociated at P0 and stained after 9 days in vitro. (B–D) Dissociated amacrine cells, plated at P0, when subset markers are not detectable, begin expressing subtype-specific antigens by 9 days in culture. Expression of GlyT1 (B), GAD65/67 (C), and NPY (D) were detected in subsets of syntaxin-1$^+$ amacrines. None of these markers was detectable at P0. (E) The fraction of cells undergoing their final S-phase at E14 (white columns), or E17 (black) is plotted for each subset marker. To account for center-periphery differences in birthdate, the *in vivo* columns (first pair of columns in each graph) use an average of values in center and periphery.

Table 1

List of Primary Antibodies Used in the Current Study

Antigen	Immunogen	Host	Working dilution	Source	Catalog no.
Bm-3a	Ami no acids 186–224 of Bm-3a fused to T7 gene 10 protein	Mouse	1:500	Chemicon	Mab1585
Chx10	Recombinant N-terminal amino acids 1–131 of human Chx10 conjugated to GST	Sheep	1:300	Exalpha	X1180P
Syntaxin (HPC-1)	Synaptosomal plasma-membrane fraction from adult rat hippocampus	Mouse	1:500	Sigma	S0664
Choline acetyltransferase (ChAT)	Purified ChAT from human placenta	Goat	1:200	Chemicon	AB144P
Neuropeptide Y (NPY)	YPSKPDNPGEDAPAEDMARYYSALRHYINLITRQRY	Rabbit	1:1000	Bachem	T-4069
Tyrosine hydroxylase (TH)	Purified TH from rat pheochromocytoma	Rabbit	1:500	Chemicon	AB152
Glutamate Decarboxylase Gad65/67	Peptide [C]DFLIEEIERLGQDL from rat GAD65	Rabbit	1:1000	Chemicon	AB1511
Glycine transporter 1 (GlyT1)	Peptide from C-terminus of rat GlyT1, AG994	Goat	1:5000	Chemicon	AB1770
Vesicular glutamate transporter 3 (Vglut3)	Peptide from rat Vglut3, AG320	Guinea pig	1:2500	Chemicon	AB5421
Ebf	C-terminal peptide of the Ebf-1 protein (NGNSLQAISGMIVPPM)	Rabbit	1:2000	Gift from R. Reed	

Table 2

Percentage of subset amacrine cells within total amacrine population of INL in center retina.

Type of cells	INL ACs%
Syntaxin	100.0%
ChAT	7.8%
NPY	11.7%
TH	0.9%
GAD65/67	42.4%
Vglut3	4.6%
GlyT1	41.3%
Ebf	48.5%